Energy Conversion and Management 183 (2019) 689–697

Contents lists available at ScienceDirect

Energy Conversion and Management

journal homepage: www.elsevier.com/locate/enconman

Thermal performance and surface analysis of steel-supported platinum nanoparticles designed for bio-oil catalytic upconversion during radio frequency-based inductive heating

Jacob Bursavich[a], Mohammad Abu-Laban[b], Pranjali D. Muley[a], Dorin Boldor[a,*], Daniel J. Hayes[b]

[a] Department of Biological & Agricultural Engineering, Louisiana State University Agricultural Center and A&M College, Baton Rouge, LA 70803, United States
[b] Department of Biomedical Engineering, Pennsylvania State University, Old Main, State College, PA 16801, United States

ARTICLE INFO

Keywords:
Induction heating
Supported nanocatalyst
Coking
Biomass conversion
Catalytic upgrading

ABSTRACT

A catalyst is designed for use in radio frequency (RF) induction-based biofuel upconversion. Stainless steel spheres are functionalized with Pt-nanoparticles through the use of a silane linker. These spheres are characterized via XRD, FTIR, SEM/EDX and XPS followed by generation of heating profiles in an RF induction heater. The high electric conductivity of the steel balls results in rapid heating which creates a positive temperature gradient across the surface with temperatures of the steel balls reaching 300 °C in under 20 s. Using a minimum of 3% power (150 W), temperatures over 525 °C are achieved within 150 s in a single steel ball experiment. A steel bed experiment is performed to simulate an induction-based catalytic upconversion of biomass pyrolysis vapors which indicates that temperatures over 195 °C are achieved in as little as 300 s using 5% power (250 W). Melting and degradation of the Pt nanoparticles is evident with repeated heating at temperatures of 525 °C and above, fortunately, typical catalysts designed for upconversion of pyrolysis oils are operating well below these temperatures. This form of heating has a potential to mitigate the effects of coke deposition on catalyst surface, which is a pressing issue during up-conversion of pyrolysis oil and various petrochemical processes.

1. Introduction

Catalyst deactivation and regeneration is a significant concern for most industrial processes in the multi-billion-dollar catalyst market. All catalysts eventually decay, and the mortality rate depends on the catalyst and the process in which it is used. Catalysts used for hydrocracking may only be viable for a matter of hours; on the other hand, certain iron-based catalysts used to generate ammonia can be reused for 5–10 years [1].

Coke deposition on catalysts like zeolites in the catalytic cracking of bio-oil makes up-conversion expensive for this process. Upconversion refers to a general increase in heating value of the product. This can be done in a number of ways, including the removal of oxygenated molecules, such as phenolic compounds, and by reducing the moisture content of the bio-oil. The rapid coke formation mechanism was reported to occur via two pathways: (i) heavy coke fraction from polycondensation and linking of aromatic compounds leading to a heavy-coke fraction, and (ii) formation of oxygen-containing coke leading to a lighter fraction [2,3].

Coke formation over acidic sites at temperatures lower than 200 °C usually occurs via condensation of reactants due to their affinity for adsorption, followed by reactions between the adsorbed species to form a large network of carbon chains [4]. The retention of the coke molecules, especially in microporous catalysts, is due to the steric hindrance within the pores of the catalyst.

Efforts to mitigate the formation of coke molecules include the use of catalytic coating to convert coke to carbon oxides by reaction with steam [5]. In addition, neutralization of external acidic sites on zeolite catalysts to prevent coke adsorption has been reported with the use of alkali molecules such as MgO and 2,4-dimethylquinoline [6]. These agents help prevent the growth of filamentous carbons on the surface but are ineffective in preventing the diffusion of the carbon polymers into the catalyst. Chemical agents like SiO_2 can be used to mitigate the condensation of coke molecules on the surface as well as their diffusion into the particle [7,8]. While several studies have looked at the mitigation of coke formation, there is little understanding of the effect of the surface catalyst temperature and the role it plays in the adsorption of coke molecules. Generally, adsorption is exothermic and an increase in temperature leads to a decrease in adsorption. However, the condensation of molecules on the surfaces can also be due to the

* Corresponding author.
E-mail address: dboldor@agcenter.lsu.edu (D. Boldor).

https://doi.org/10.1016/j.enconman.2019.01.025
Received 26 November 2018; Accepted 6 January 2019

temperature gradient normal to the surface of the catalyst. A negative temperature gradient can lead to a faster rate of the coke adsorption. Hence, the heating method of the catalyst reactor can play a significant role in the formation of fouling compounds on the surface sites that reduce the catalysts longevity.

The significance of producing high-energy biofuel is more apparent in the face of increasing atmospheric CO_2 levels and the resource limitations naturally present in the use of fossil fuels. High oxygen content of biomass improves its biodegradability but lowers its energy potential. Catalyst-based hydrodeoxygenation (HDO) reactions in bio-oils are used to reform oxygenated components into water and hydrocarbons and typically save valuable carbon mass through the direct hydrogenation of C—O bonds [9]. HDO catalysts often are metallic-based using transition and noble metals [10–12]. While both have been studied in reference to the promotion of HDO reactions in bio-oils, to various degrees of success, all tend to suffer from coking-related deactivation [13].

Induction heating is an efficient method of heating that involves the passing of an alternating current through a metal coil which induces an alternating magnetic field as discovered by Lorentz, Ampere and Maxwell [14]. This alternating magnetic field induces eddy currents on any electrically conductive load placed within the volume of the coil, and/or hysteresis loss in magnetic loads [15–17]. Direct resistance from these effects result in heating of the load. Since the heat originates from the load itself, this method yields rapid heating rates with minimal losses to the surroundings during induction. Recently, induction heating has been explored for various applications including pyrolysis and pyrolytic vapor upgrading [18–20]. The electromagnetic phenomena involved in induction heaters can be described using Maxwell's equations [21].

To apply this heating method to the issue of coke formation, the design of a metallic-supported catalyst is needed in which the heat directly emanates from the surface to deter condensation of unsaturated hydrocarbons and aromatics that form coke. While some catalysts contain material with high magnetic permeability and electric permittivity, these quantities are typically too small to induce a large heating effect in the catalyst bed. Most catalytic upgrading processes require a temperature of at least 200 °C, especially if the reaction is occurring in the gaseous phase, to prevent oil condensations in the catalyst bed. Therefore, a macro-sized support is needed to anchor the active catalysts and maintain high temperatures for the bed.

In this study, we propose a steel-supported Pt-nanoparticle system heated through an induction-based system. Noble metal catalysts generally are typically too expensive for fuel production from biomass due to the relatively economic cost of fuels [22]; however, due to its known catalytic properties, platinum was chosen in this instance as a testing model for RF-based pyrolytic upgrading. Alternative, cheaper metallic catalysts could be substituted for larger-scale operations. The hydrodeoxygenation (HDO) catalytic properties of platinum have led to its use in various applications [23,24], such as the removal of trans fatty acids by hydrogenation in cottonseed oil [25], the electro reduction of oxygen in fuel cells [26], the hydro-de-chlorination of tetrachloromethane [27], and the HDO of lignin containing biomass [28]. The popularity of nanocatalysts for catalytic reactions is a result of their high surface area retention. Platinum reduction reported in Tang et al. [29] is used to synthesize Pt nanoparticles and deposit them onto the surfaces of steel balls. Steel is an electric conductor that heats up directly under RF fields via the Joule heating effect from the induced eddy currents. The use of common steel balls provides a high surface area for catalytic sites, but was also chosen to promote the idea of valorizing industrial by-products, such as converter slag and blast furnace sludge [30]. Industrial by-products with metallic content potentially be used as a substitute in RF heating. One of the novel purposes of this method would be to establish a positive temperature gradient across the surface of the catalyst in order to deter coke and oil condensation (Fig. 1).

To our knowledge, this work is the first report on the heating profiles of stainless steel (SS) balls functionalized with Pt nanoparticles in an induction heater, and on the surfaces analysis after Pt-modification. Generally, the process of making bio-oils involves breaking down organic complex molecules in biomass material into smaller molecules, via a thermo- or bio-chemical reaction [31]. Multiple factors have put the production of biofuels to the forefront as an energy source. Government regulations, the high cost of petroleum and its environmental costs, as well as its production in unstable parts of the globe, have all led to in-depth studies into this field and increasing its efficiency [32]. However, pyrolysis produces a significant amount of water and oxygen in the final product, which renders it unusable as transportation fuel. Through the hydrodeoxygenation of the organic compounds over Pt-based nanocatalysts, the low energy value of the oil can be increased [28].

2. Experimental section

2.1. Materials

Type-316 stainless steel (SS) spheres (0.1875″ and 0.25″ diameter) and type-316 steel foil (0.004″ thick) were purchased from McMaster-Carr®, $N_2PtCl_6{\cdot}6H_2O$ and CH_2O were both purchased from Sigma-Aldrich Co. LLC., and NaOH was purchased from Thermo Fisher Scientific Inc. $C_6H_{16}O_2SSi$, purchased from Gelest, Inc. (Morrisville, PA), was used as the silane linker in preparation of reducing the Pt onto the SS surfaces and custom-made quartz tubes were ordered from Technical Glass Products, Inc. (Painesville Twp., OH). All chemicals and reagents purchased were analytical grade and used without any additional treatment or purification. The biomass that was used was pinewood sawdust from kraft wood that was obtained from the machine shop in the biological engineering department at Louisiana State University.

2.2. Preparation of Pt reduced-stainless steel spherical catalysts

The silane functionalization of the steel balls was based on Gelest's Applying a Silance Coupling Agent method [33]. SS balls were rinsed with DI water and ethanol and left to dry in atmospheric conditions for between 1 and 2 h at 100 °C. The surfaces of the balls were then modified with an oxide layer via plasma oxidation under vacuum for 30 s. The plasma oxidized steel balls were then immersed in 2% silane linker in 95% ethanol solution and agitated between 2 and 3 min at room temperature (approximately 25 °C) under atmospheric conditions. The silane solution was then decanted and the steel balls rinsed with ethanol and left to dry overnight, followed by a DI water rinse and further drying within an oven. An alternative approach for comparison that we investigated was to heat the steel balls to 1000 °C to allow for oxidation to occur and blacken the surface to increase the surface area available for nucleation and growth.

2.3. Reduction of Pt onto SS surface

Following the silane functionalization, Pt reduced onto the SS surface based on a method by Tang et al. [29] Briefly, a 20 mM aqueous solution of H_2PtCl_6 was prepared and mixed with the SS balls and the pH was raised to 12 by gradual addition of a 0.1 M NaOH solution. The solution was then heated to approximately 90 °C, under vigorous stirring conditions. Excess formaldehyde (36.5%) was then added at a 10:1 molar ratio, with respect to $[PtCl_6]^{-2}$. The reduction of chloroplatinic to platinum was observable as the color of the solution visibly changed from yellow-orange to black (Fig. S1). The steel balls were then rinsed with hot DI water (approximately 65 °C) until the filtrate tested negative for formation of a white precipitate using 0.1 M silver nitrate solution. This was followed by overnight heating in an oven at 150 °C. After heating, the balls were allowed to cool to room temperature

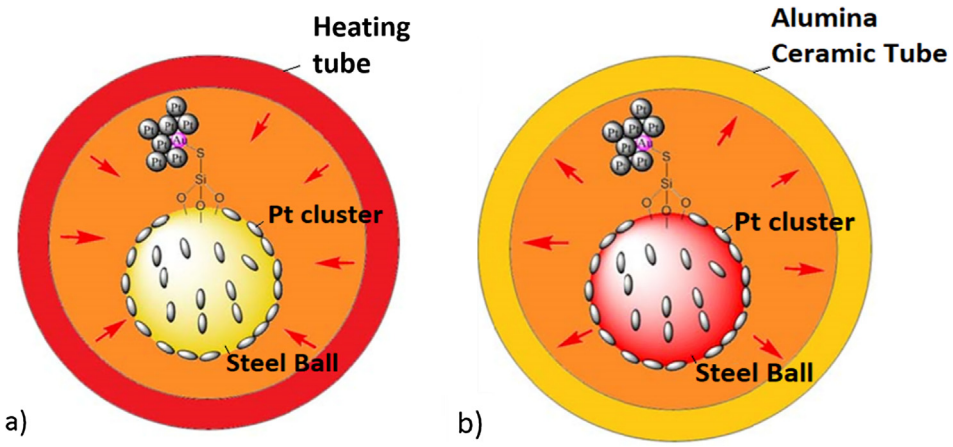

Fig. 1. Heat transfer flow from (a) tube walls toward the interior in conventional heating systems, and (b) from the steel ball surfaces to the tube walls. (Not to scale; only one functionalized-steel ball is shown for illustration purposes; arrows indicate the heat flux).

before testing in the induction heater. This process was repeated with silica balls for use as a control.

2.4. Characterization of Pt reduced-stainless steel spherical catalysts

Scanning Electron Microscopy-Electron Dispersive Spectroscopy (SEM-EDS) measurements were conducted with a JSM-6610 LV SEM equipped with EDS operated under high vacuum at beam voltage of 20 kV. SEM-EDS was used to quantify the surface Pt as well as Au, relative to other species, and to image the Pt nano-clusters that were formed. Fourier Transform Infrared Spectroscopy (FTIR) measurements were taken using a Bruker Tensor 27 FTIR machine to verify the adherence of the silane linker to the stainless-steel balls. During the FTIR analyses, collection of the absorption spectra was performed and the background signal of the steel was subtracted from the final spectra. Due to the geometrical nature of the SS balls, most of the x-ray analyses utilized were incompatible with the FTIR analyses. X-Ray Diffraction (XRD) measurements were taken using a Panalytical Empyrean multipurpose diffractometer equipped with PreFIX (pre-aligned, fast interchangeable X-ray) modules using CuKα radiation. The samples were measured between $20^\circ < 2\theta < 100^\circ$ at Kα = 1.54 nm, and the Scherrer formula was used on the first peak to determine the crystal size of the Pt. XRD analyses were performed on Pt nanoparticles that had been reduced in solution. Photoelectron Spectroscopy (XPS) measurements were conducted using a Kratos AXIS 165 XPS/SAM system equipped with a Scanning Auger Electrostatic gun (LaB6 filament, 15 kV, 100 μA). All of the XPS peaks were calibrated to atmospheric carbon 1s peak at 284.5 eV.

2.5. Heat profile generation via RF induction heating

The platinum functionalized SS balls were heated with an HFI model induction heater (RDO Induction L.L.C., Washington, New Jersey). Heating was carried out at the following power levels-150 W (3%), 250 W (5%), and 350 W (7%). Profiles were generated through the individual heating of different-sized, steel balls of 0.1875″ and 0.25″ diameter. In order to record the surface temperature, the balls were placed into a small, ceramic crucible which was then placed within a vertical coil (circular winding, 3 turns, 1.0″ I.D.) attached to the induction heater. Heating was carried out for three minutes during each run (Fig. 2, top right inset). The temperature was monitored and recorded in real time using a FLIR A40R IR camera (FLIR Systems, Inc., Wilsonville, Oregon) connected to ThermaCAM Professional 2.9 thermal data acquisition software (FLIR Systems, Inc., Wilsonville, Oregon), as illustrated in Fig. 2. The obtained emissivity values were averaged from three attempts through trial and error method and compared to a thermocouple. Additionally, steel balls pre-oxidized at 1000 °C to create a uniform oxide film surface were also measured with and without Pt reduction to provide a basis for surface heating comparison. A detailed schematic for pyrolysis and upconversion process is shown in Fig. 2b.

Initial data on deoxygenation performance was obtained by pyrolysis of sawdust biomass based on the work reported by Muley et al. [34] and Henkel et al. [19], 10 g of dried sawdust was packed inside a 304 SS tubular reactor. This biomass reactor was suspended within an RF induction coil (10-loop, rubber-insulated copper coil, 285 mm in length and 59 mm ID), connected to an RDO LFI-model power supply (35–100 kHz) (Fig. 2, top left inset). The biomass reactor was connected to a 5% H_2/95% N_2 gas line, and to the catalyst bed in the quartz tube in series. One hundred grams of the smaller (0.1875″) steel balls functionalized with Pt were packed inside the quartz tube, which was maintained at 196 °C for the duration of the pyrolysis. This temperature was selected as the lowest one practically achievable in this system, that is also relatively close to the first reduction peak of Pt (around 167 °C), described in our prior work [28].

3. Results

3.1. Surface analysis

The platinum nanoparticles on the SS surface were observed using Scanning Electron Microscopy (SEM) which revealed crystalline nanoparticle formation, along with aggregations (Fig. 3, top row). The smallest crystals observed ranged from 20 to 50 nm in diameter, while some clusters were of the order of micron. Upon heating at the three power levels (3%, 5%, and 7%) within the small vertical coil, SEM imaging revealed melting and degradation of the Pt nanoparticles at certain temperatures (Fig. 3, bottom row).

At 3%, the maximum temperature reached was approximately 525 °C (~800 K) and minor degradation was observed. At higher power levels significant melting and merging of nanoparticles into larger clusters was observed. While the melting point of Pt is 1768 °C (2041 K), the melting points of materials generally decrease as their size decreases [35]. Fortunately, for the up-conversion of pyrolysis oil, temperatures of 525 °C (800 K) are extreme and unnecessary.

The average crystal size determined from the XRD peak associated with miller index (111) was 21 nm (Fig. 4a). The remaining peaks and their respective miller indices associated with the face-centered cubic structure of the Pt particles are also labeled at their respective angles. EDX verification of Pt (and the gold seeded nanoparticles) on the surface of the balls (Fig. 4b) was used to quantify the Pt deposition (Fig. 4c) relative to the surface compounds of the steel and for

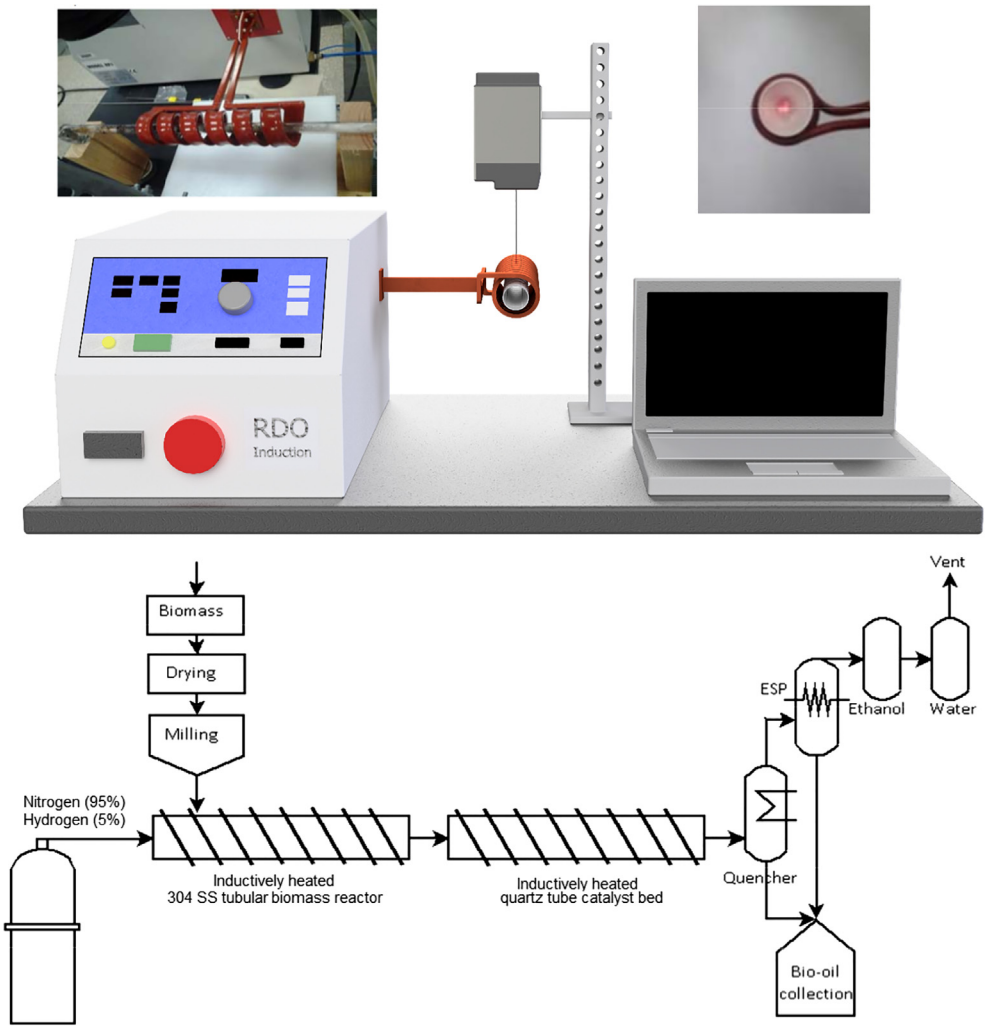

Fig. 2. (a) Overall setup of RF heating of steel balls with temperature measurements using IR camera. Top left inset: RF coil and quartz tube for larger, horizontal coil setup. Top right inset: Ceramic crucible with individual steel ball inside used in small, vertical coil setup. (b) Schematic of pyrolysis setup with upgrading.

observing and comparing any changes in the Pt concentration on the surface of the balls before and after heating.

FTIR analysis was used to confirm the presence of silane bonding to SS balls surface. The peaks for Si—O-metal (1000–900 cm^{-1}), Si—O—Si (1130–1000 cm^{-1}), SiCH3 (1275–1245 cm^{-1}), C—H (3000–2700 cm^{-1}), and O—H (3000–3500 cm^{-1}) were identified. The S—H peak, which is a relatively weak peak, was not observed (Fig. 4d). The steel balls investigated included two different sized, stainless steel as material, and the pre-oxidized steel balls. Between the stainless and pre-oxidized steel balls, it can be deduced that the pre-oxidized balls retain a much larger Pt quantity on their surface. This effect may be attributed to roughness induced as a result of oxidization, reflecting an increased surface area and potential for nucleation and growth of Pt nanoparticles.

To verify the purity of the reduced Pt species, XPS analysis was performed (Fig. S2) which indicated via spectral deconvolution the presence of two Pt species-Pt^0 and Pt^{2+} with relative percentages of 57%and 43% respectively (Table S1). The high Pt/Cl ratio of 13.3 indicated low presence of unreduced Pt salt, suggesting the Pt^{2+} to be primarily present in the form of PtO.

Another trend worth noting is the decrease in surface concentration of Pt after heating in all versions of the steel balls investigated. In the case of the smaller balls (Fig. 4c), when heated twice consecutively at 3% power, we observe a downward trend in Pt quantity after each heat application. One theory behind these phenomena is that of differential diffusion. With heating of the surface, the stainless steel begins to oxidize resulting in an uneven layer with porous pathways across the surface [36]. The concentration gradient now established results in the migration of the Pt deeper into the surface. Furthermore, heat generation by means of eddy currents is slightly higher at the interface of two metals [37], although sometimes difficult to detect [38]. This increased heat results in a softening of the support metal at the interface which may further promote Pt migration toward the interior of the support.

3.2. Heating profiles

The emissivity values for each steel ball are listed in Table S2 in the supplementary information. Fig. 5(a–c) shows the temperature plots of the platinum coated balls and the control within the small vertical coil (circular winding, 3 turns, 1.0″ I.D.) at 3 different power levels. Of note, the temperature of the steel balls increased to ~300 °C (573 K) in less than 20 s and no observable differences were noted in the heating profiles due to Pt on the surface of the steel balls. Similar trends were also observed in the temperature profiles for both the smaller (0.1875″) and larger (0.25″) steel balls. The maximum temperatures reached at the higher powers were much higher than necessary for catalytic activity which typically ranges between 327 °C (600 K) and 527 °C (800 K) [39].

A control study to evaluate the heating effect of the Pt nanoparticles alone used silica beads as substrate. Both the bare silica and the Pt-

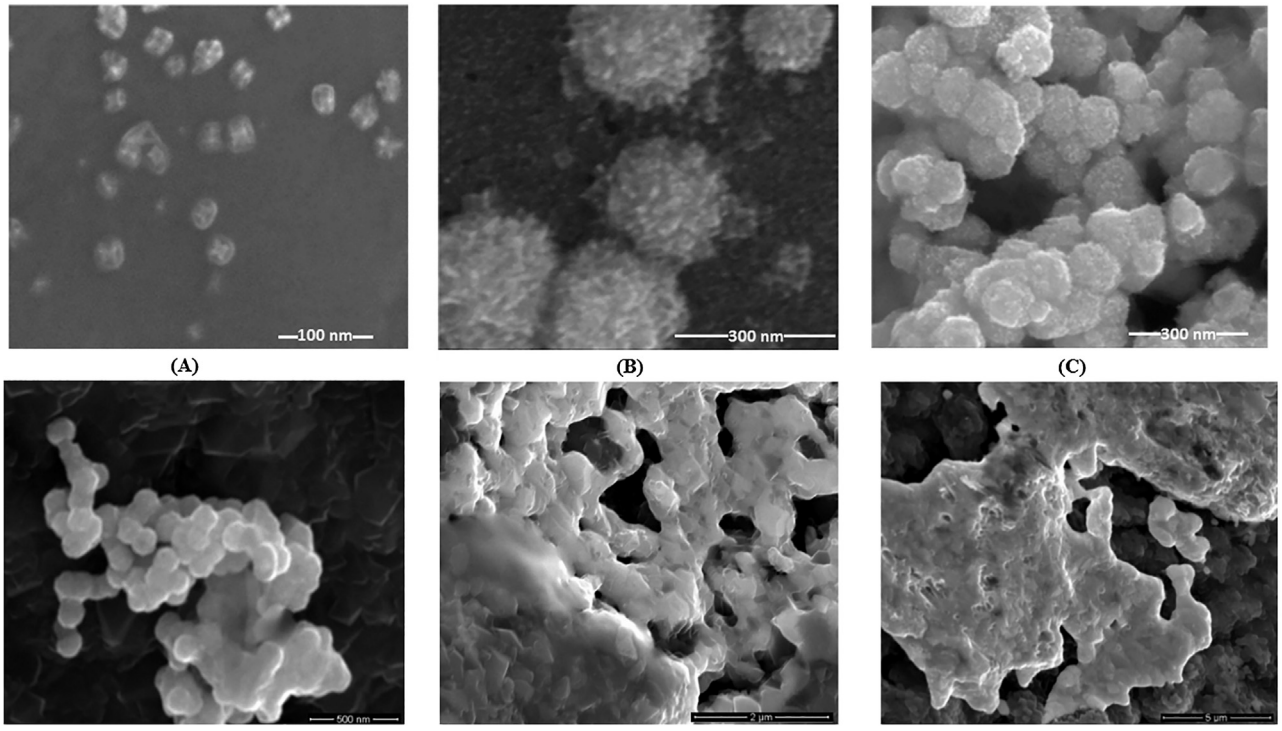

Fig. 3. (A)–(C) SEM imaging, from high to low magnification (350 k, 200 k, 150 k respectively) of nanoparticles forming on steel surface and aggregating to form nano-scale islands, prior to heating. (D)–(F) SEM imaging from high to low magnification (65 k, 25 k, 8 k, respectively) of steel surfaces after heating at different power levels. At the higher levels, melting of nanoparticles can be observed.

modified silica beads remained at room temperature under an RF field (Fig. 6 – top), which is expected as the Pt nanoparticles themselves have insignificant mass compared to the beads and thus do not possess enough impedance to generate heat in the configuration used. At the same time, the heating is clearly visible in IR images of Pt-seeded steel balls (Fig. 6 – middle and bottom).

All the temperature profiles above were normalized to 25 °C (298 K) and fitted into a simple exponential rise to maximum (Eq. (1)) correlation with 2 parameters (a and b):

$$\boldsymbol{T}(\boldsymbol{K}) = 298 + a * (1 - e^{-b*t(s)}) \quad (1)$$

The parameter values for each plot are recorded in Table S3.

Even at low powers, the steel balls reached significantly high temperatures as a result of the applied RF field. From the above heating profiles, the heating rate of the oxidized steel balls appeared faster than that of the SS balls of the same size. The b parameter, or the decay constant, fitted for each of the profiles does in fact have a larger value for the oxidized version (0.028–0.0296) than that of the non-oxidized version (0.0105–0.0209). Since the heat generated originates from the direct resistance of the eddy currents circulating on the surfaces, the heat generated from the oxidized steel balls is much greater due to its lower electrical conductivity relative to its non-oxidized form [40]. An increase in the electrical resistance is also expected as a result of the increased surface roughness with oxidization.

To investigate the ability of the balls to heat a potential catalyst bed to reasonable temperatures, the oxidized-film steel balls, which showed the fastest heating rate, were loaded into a quartz tube and suspended within a larger coil (cylindrical winding, 6 turns, 2.0″ I.D.). The temperature profiles at the different power levels are presented in Fig. 7 with the fitting parameters listed in Table S4. With the larger loading, the same applied power at 5% resulted in a more moderate temperature increase compared to the small coil crucible experiment. Overall, higher powers were necessary to gain higher bed temperatures. Despite this, even at the lowest power (5% or 250 W), the maximum temperature reached at the lower range generally required for catalytic upgrading (Fig. 7). The maximum steady state temperature for each experiment in the larger coil with multiple steel balls was correlated to the power using a 3-parameter exponential rise to maximum (Eq. (2). Fig. 7 inset)

$$\boldsymbol{T}(\boldsymbol{K}) = y_0 + a * (1 - e^{-b*t(s)}) \quad (2)$$

The GC–MS spectra of the oil without up-conversion and that passed through the steel-Pt bed at the lowest temperature (470 K or ~200 °C) are shown in Fig. S3. The peak locations and intensities look roughly similar, and after identifying and classifying the compounds, any differences in the chemical make-up of both samples (Fig. 8) were largely insignificant based on their proportional weights in solution. A statistical one-tail t-test ($\alpha = 0.05$) between the two groups for each organic compound class suggested no significant variations. The only exception to this was the ketones group which increased from 12 wt% to 18 wt% but was disregarded as inconsequential due to the results of the elemental analysis. The molar O/C ratios of the organic phase in the oil were determined to be 1.58 for the bio-oil without upgrading, and 1.64 for the oil treated with Pt-steel.

4. Discussion

To investigate the efficiency of heating catalyst supports directly with an RF induction heater, we successfully synthesized a steel-supported Pt-nanoparticle system functionalized using a silane coupling agent. The high electric conductivity of the steel balls resulted in their rapid heating, which created a positive temperature across the surface. This form of heating has the potential to mitigate the effects of coke formation, such as in the up-conversion of pyrolysis oil [28]. With the use of a bed of functionalized steel balls, the longer coil and quartz tube experiment reached high enough temperatures for upgrading with minimum power requirements from the RF induction heater. In the small coil experiment, within 150 s, and at 7%, 5%, and 3% power, temperatures over 1200 K (~925 °C), 900 K (~625 °C), and 800 K (~525 °C) were reached, respectively. More moderate temperature

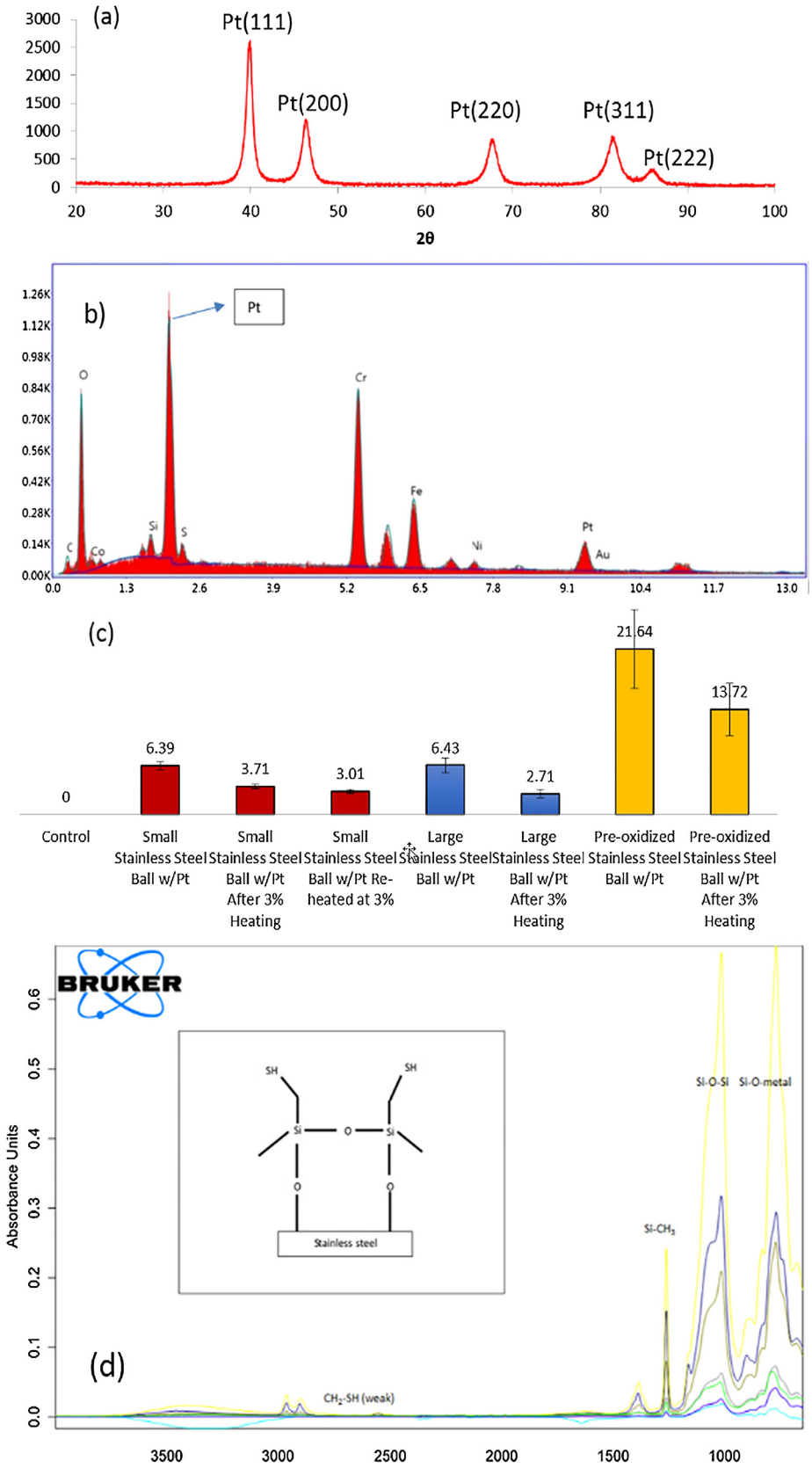

Fig. 4. (a) X-ray diffraction spectra collected for PtNPs in solution, (b) EDX spectra for a Pt-reduced steel surface, (c) Average wt% of Pt for the different steel substrate with and without heating, (d) FTIR spectra confirming presence of silane bonding to the surface of the stainless steel balls.

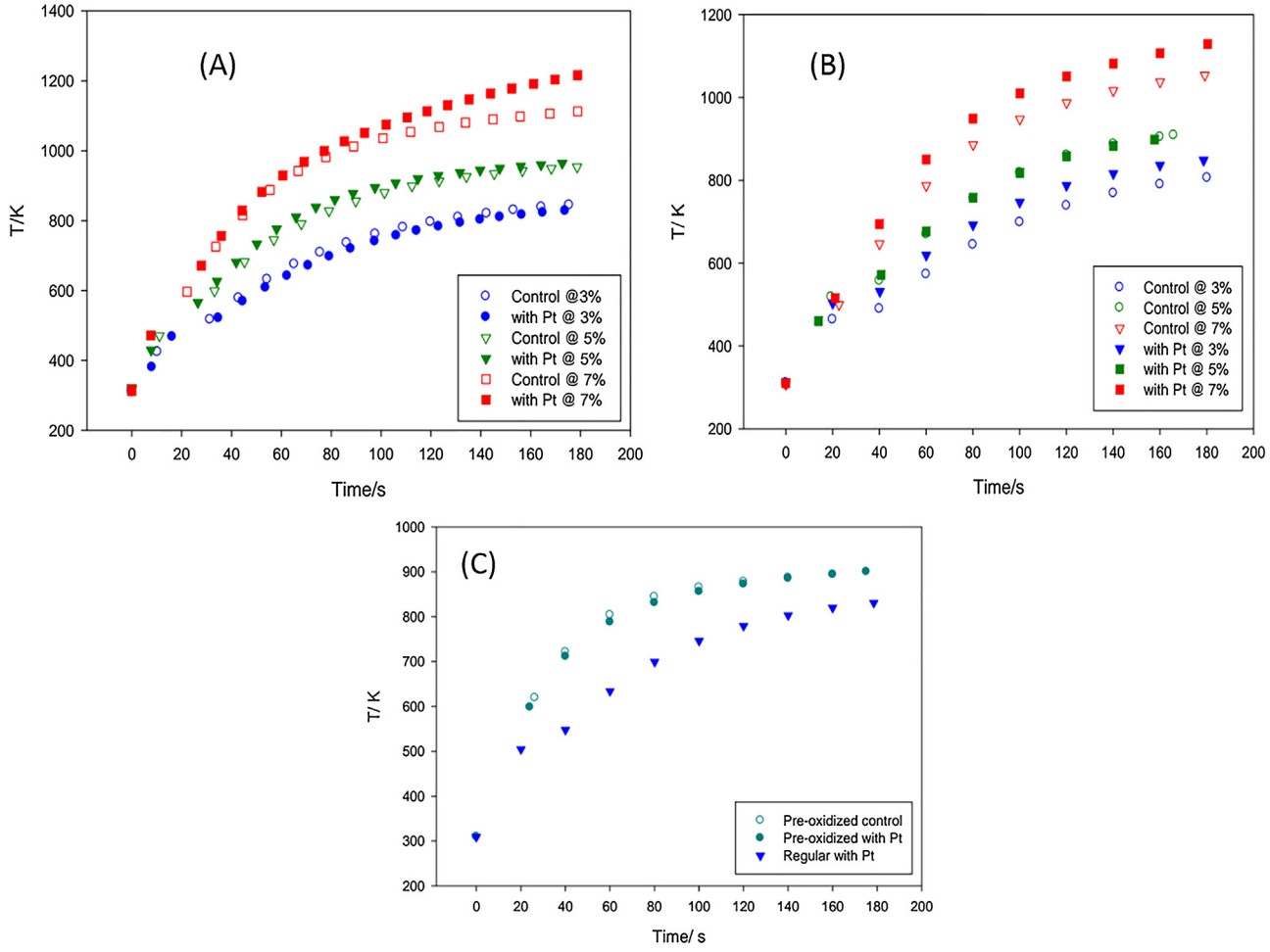

Fig. 5. (a) Temperature plots comparing smaller steel balls with Pt and without, at 3 power levels: 3%, 5%, and 7% (of 5 kW max). (b) Temperature plots comparing the heating profiles of the larger sized steel balls. (c) Temperature plots for pre-oxidized small steel balls with and without Pt, compared also to their stainless counterpart at 3% (150 W) power levels.

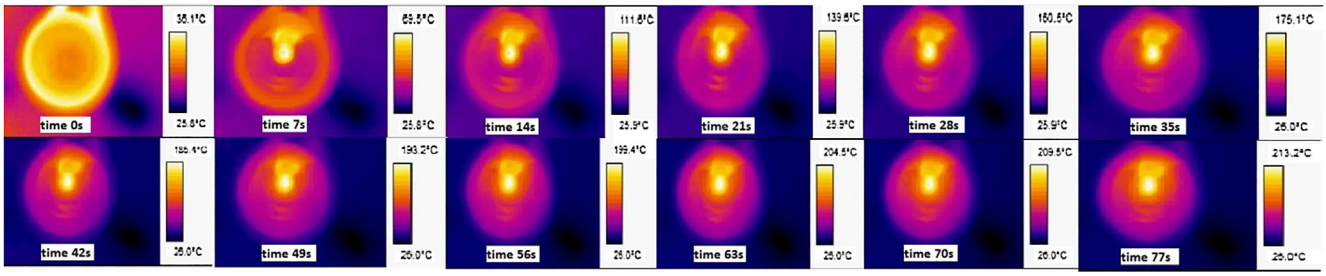

Fig. 6. Top: Real-time IR images of Pt-seeded silica ball under RF heating. Middle and Bottom: Real-time IR images of Pt-seeded steel ball under RF heating. Time snapshots are denoted in the overlays. Note difference in temperature scales.

increases were seen in the large coil with more steel ball loading than compared to the small coil with a single steel ball study. Within 300 s, at 15% (750 W), 10% (550 W), and 5% (250 W) power, temperatures of 650 K (~375 °C), 575 K (~300 °C) and 470 K (~200 °C) were achieved. Notwithstanding, the lower temperature obtained in the large coil study at a minimum power of 5%, or 250 W, are sufficiently high for many catalytic processes. Due to these factors, the quartz tubes were not insulated, as additional thermal insulation would reduce the power requirements necessary below 3% power, the minimum power at which the equipment was operational.

The use of steel scaffolding for direct functionalization of catalytic groups and as a heat source is a novel approach within the realm of induction-based pyrolysis. Surface functionalization of the steel ball or other metallic supports introduces new possibilities of maximizing catalytic surface area and the generation of modified catalytic responses, with the internal heat source providing a unique approach to combating the negative effects that coking has on catalytic outputs. One major drawback with this particular design is the limited surface area per volume available with the use of the steel balls. The mass of the Pt on the surface of the balls for the up-conversion totaled less than half a gram, while the biomass loading was 10 g. This large feed-to-catalyst ratio inhibits significant upgrading. Increasing the catalyst load may be one solution, but not a practical one due to the weight of the steel balls needed. Moreover, the calculated residence time for the catalyst bed was determined to be 4.25 s which, coupled with the small catalyst area available, further disadvantages any catalytic adsorption and activity. A

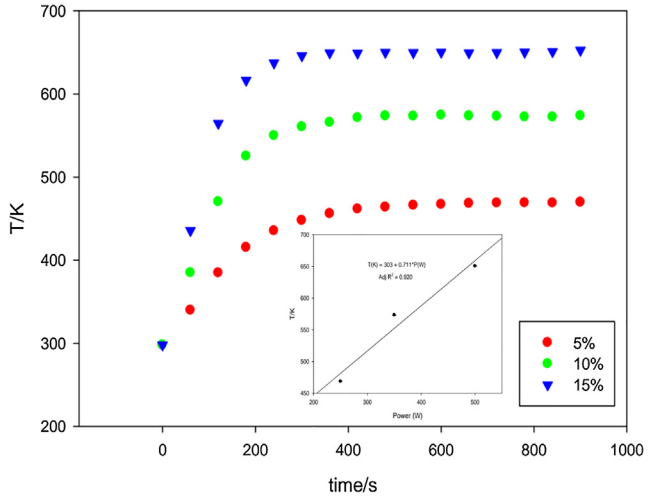

Fig. 7. Heating Profiles for the smaller oxidized steel balls packed bed at 5% (250 W), 10% (500 W), and 15% (750 W) power. Inset. Maximum steady state temperature (K) as a function of induction heating power (W).

possible solution would be to increase the length of the reactor to mitigate the short gas-catalyst contact time. A more practical alternative would be a repeat of the design on a more porous steel structure, such as wool or a mesh structure, to seed and grow the catalyst particles and maximize both the surface area available and the number of Pt catalytic sites. Temperature studies to ensure these structures maintain a high enough catalyst bed temperature would also be required. The lack of significant hydrodeoxygenation effect can be attributed also to the relatively low temperature used in these tests (even though close to the Pt reduction peak of 167 °C, it is not enough for significant hydrogenation which occurs at higher temperatures). In a separate study [16], we have shown the effectiveness of steel ball supports mixed with Pt/Al_2O_3 catalyst pellets in both upconversion of bio-oil vapors and reduced coking. Future modifications to directly-functionalized steel supports, such as Pt/Al_2O_3 nanoparticles directly functionalized to steel supports, would provide interesting comparative data.

Platinum group metals, such as platinum, palladium and rhodium, are usually chosen for their high chemical stability and known catalytic activity. Due to their low magnetic permeability, low resistivity as well as the small quantity used, in comparison with 316 SS, the platinum loading should generate negligible amounts of heat in the system, which was confirmed by the silica ball study; however, localized, minor heat generation at the platinum site may influence the catalytic reactions that occur. Further investigation is required to determine the relevance of this micro-localized heating on their catalytic activity. Variations in both the catalytic group and the type of steel support may also improve the efficiency of catalytic responses in this novel system. Silane coupling was chosen as it is a common and relatively easy bonding procedure which can be replicated on a number of different materials other than steel. The proposed system is reusable over a number of catalytic cycles; however, it was observed that the quantity of Pt on the surface of the steel balls was reduced over time. Alternative approaches to traditional silane coupling such as thiol and phosphate primers or aryl diazonium coupling agents should be investigated as they may have influence on the reduced surface concentration of the surface metal observed over repeated heating cycles. At temperatures of 525 °C (800 K) and above, melting and degradation of the nanoparticles was observed in SEM imaging, therefore this catalytic system is optimized for temperatures below these values. These values, fortunately, correspond to typical temperatures required not only for the up-conversion of pyrolysis oil, but also for many other catalytic processes. The easily, adaptable system proposed in this study can be easily modified to incorporate alternative catalytic surface groups to investigate if currently used catalytic systems could be improved through either the reduction of coking effects or possible novel modifications to the catalytic mechanism due to internal heat generation through induction.

An indirect result of this study was the observation of the possible migration of surface Pt deeper into the interior of the steel balls after a series of heating cycles. This result appeared to decrease the catalytic efficiency of the system but might have usefulness as a novel method for fabricating precisely-layered, metal alloys in which the structure of the prefabricated geometry of the metal is maintained during the fabrication process. Multi-layered alloys may have interesting mechanical and/or catalytic properties that could be advantageous for a multitude of applications. As this was out of the scope of our investigation, further research would be required to confirm whether internal deposition of the platinum nanoparticles within the interior layers of steel support was, in fact, occurring and whether or not this could be used as a feasible fabrication method for generating alloys.

5. Conclusions

A nanocatalyst was designed for biofuel upconversion in (RF) induction reactors. Stainless-steel spheres with high electrical conductivity were functionalized with Pt-nanoparticles using a silane linker. The high conductivity of the steel resulted in rapid heating inside the reactor creating a positive temperature across the surface. High heating rates were observed with the spheres reaching 300 °C in under 20 s. Heating was observed to be highly efficient, using a minimum power of 3% (150 W), to reach 525 °C in single steel sphere experiments within 150 s. Steel bed experiments, performed to simulate induction-

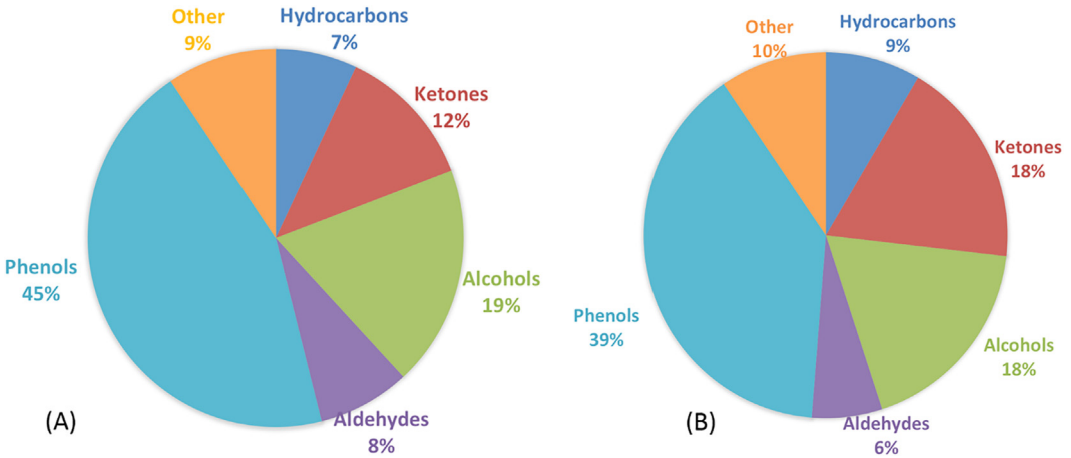

Fig. 8. Chemical composition of pyrolysis oil without upconversion (a), and with upconversion with Pt/Steel.

based pyrolysis of biomass with upconversion in larger beds, indicated that temperatures over 195 °C were achieved in 300 s using 5% power (250 W). SEM indicated melting and degradation of the Pt-nanoparticles when repeatedly heated at temperatures of 525 °C and higher; fortunately, catalysts designed for upconversion of pyrolysis oils operate well below these temperatures.

Acknowledgements

This work was funded by the National Science Foundation (NSF) (#CBET 1437810). Partial support was also provided by the LSU Agricultural Center, the Department of Biological and Agricultural Engineering at LSU, USDA NIFA via Hatch Program, and the Louisiana Board of Regents (award # LEQSF (2015-17)-ENH-TR-01). The authors would like to thank Dr. James Spivey for his technical support and advice. Published with the approval of the Director of the Louisiana Agricultural Experiment Station as manuscript # 2018-232- 32291.

Appendix A. Supplementary material

Supplementary data to this article can be found online at https://doi.org/10.1016/j.enconman.2019.01.025.

References

[1] Argyle MD, Bartholomew CH. Heterogeneous catalyst deactivation and regeneration: a review. Catalysts 2015;5(1):145–269.
[2] Guisnet M, Ribeiro FR. Deactivation and regeneration of zeolite catalysts vol. 9. World Scientific; 2011.
[3] Ibarra Á, Veloso A, Bilbao J, Arandes JM, Castaño P. Dual coke deactivation pathways during the catalytic cracking of raw bio-oil and vacuum gasoil in FCC conditions. Appl Catal B 2016;182:336–46.
[4] Guisnet M, Magnoux P. Organic chemistry of coke formation. Appl Catal A 2001;212(1–2):83–96.
[5] Schietekat CM, Sarris SA, Reyniers PA, Kool LB, Peng W, Lucas P, et al. Catalytic coating for reduced coke formation in steam cracking reactors. Ind Eng Chem Res 2015;54(39):9525–35.
[6] Zhang B, Zhong Z, Xie Q, Chen P, Ruan R. Reducing coke formation in the catalytic fast pyrolysis of bio-derived furan with surface modified HZSM-5 catalysts. RSC Adv 2015;5(69):56286–92.
[7] Bibby DM, Howe RF, McLellan GD. Coke formation in high-silica zeolites. Appl Catal A 1992;93(1):1–34.
[8] Cheng S, Wei L, Julson J, Rabnawaz M. Upgrading pyrolysis bio-oil through hydrodeoxygenation (HDO) using non-sulfided Fe-Co/SiO_2 catalyst. Energy Convers Manage 2017;150:331–42.
[9] Zharova PA, Chistyakov AV, Shapovalov SS, Pasynskii AA, Tsodikov MV. Pt–Sn/Al_2O_3 catalyst for the selective hydrodeoxygenation of esters. Mendeleev Commun 2018;28(1):91–2.
[10] Jahromi H, Agblevor FA. Hydrodeoxygenation of Aqueous-phase catalytic pyrolysis oil to liquid hydrocarbons using multifunctional nickel catalyst. Ind Eng Chem Res 2018;57(39):13257–68.
[11] Agblevor FA, Jahromi H. Aqueous-phase synthesis of hydrocarbons from furfural reactions with low-molecular-weight biomass oxygenates. Energy Fuels 2018;32(8):8552–62.
[12] Gonzalez-Olmos R, Anfruns A, Aguirre NV, Masaguer V, Concheso A, Montes-Morán MA. Use of by-products from integrated steel plants as catalysts for the removal of trichloroethylene from groundwater. Chemosphere 2018;213:164–71.
[13] Ochoa E, Torres D, Moreira R, Pinilla JL, Suelves I. Carbon nanofiber supported Mo_2C catalysts for hydrodeoxygenation of guaiacol: The importance of the carburization process. Appl Catal B 2018;239:463–74.
[14] Purcell EM, Morin DJ. Electricity and magnetism. Cambridge University Press; 2013.
[15] Lucia O, Maussion P, Dede EJ, Burdío JM. Induction heating technology and its applications: past developments, current technology, and future challenges. IEEE Trans Ind Electron 2014;61(5):2509–20.
[16] Lupi S, Forzan M, Aliferov A. Induction and direct resistance heating. Springer; 2015.
[17] Moreland W. The induction range: its performance and its development problems. IEEE Trans Ind Appl 1973;1:81–5.
[18] Daniel DJ, Ellison CR, Bursavich J, Benbow M, Favrot C, Blazier MA, et al. An evaluative comparison of lignocellulosic pyrolysis products derived from various parts of Populus deltoides trees and Panicum virgatum grass in an inductively heated reactor. Energy Convers Manage 2018;171:710–20.
[19] Henkel C, Muley PD, Abdollahi KK, Marculescu C, Boldor D. Pyrolysis of energy cane bagasse and invasive Chinese tallow tree (*Triadica sebifera* L.) biomass in an inductively heated reactor. Energy Convers Manage 2016;109:175–83.
[20] Muley PD, Henkel C, Abdollahi KK, Marculescu C, Boldor D. A critical comparison of pyrolysis of cellulose, lignin, and pine sawdust using an induction heating reactor. Energy Convers Manage 2016;117:273–80.
[21] Trémolet de Lacheisserie É, Schlenker M, Gignoux D. Magnetism: materials and applications. Springer; 2005.
[22] Agblevor FA, Jahromi H. Aqueous phase synthesis of hydrocarbons from reactions of guaiacol and low molecular weight oxygenates. ChemCatChem 2018;10(22):5201–14.
[23] Vo TK, Kim W-S, Kim S-S, Yoo KS, Kim J. Facile synthesis of Mo/Al_2O_3–TiO_2 catalysts using spray pyrolysis and their catalytic activity for hydrodeoxygenation. Energy Convers Manage 2018;158:92–102.
[24] Cheng S, Wei L, Julson J, Muthukumarappan K, Kharel PR. Upgrading pyrolysis bio-oil to biofuel over bifunctional Co-Zn/HZSM-5 catalyst in supercritical methanol. Energy Convers Manage 2017;147:19–28.
[25] Cheng H, Dowd MK, Easson MW, Condon BD. Hydrogenation of cottonseed oil with nickel, palladium and platinum catalysts. J Am Oil Chem Soc 2012;89(8):1557–66.
[26] Chen A, Holt-Hindle P. Platinum-based nanostructured materials: synthesis, properties, and applications. Chem Rev 2010;110(6):3767–804.
[27] Bonarowska M, Karpiński Z. Hydrodechlorination of tetrachloromethane over supported platinum catalysts. effects of hydrogen partial pressure and catalyst's screening protocol on the catalytic performance. Top Catal 2012;55(11–13):846–52.
[28] Abu-Laban M, Muley PD, Hayes DJ, Boldor D. Ex-situ up-conversion of biomass pyrolysis bio-oil vapors using Pt/Al_2O_3 nanostructured catalyst synergistically heated with steel balls via induction. Catal Today 2017;291:3–12.
[29] Tang X, Zhang B, Li Y, Xu Y, Xin Q, Shen W. Structural features and catalytic properties of Pt/CeO_2 catalysts prepared by modified reduction-deposition techniques. Catal Lett 2004;97(3–4):163–9.
[30] Gonzalez-Olmos R, Anfruns A, Aguirre NV, Masaguer V, Concheso A, Montes-Morán MA. Use of by-products from integrated steel plants as catalysts for the removal of trichloroethylene from groundwater. Chemosphere 2018;213:164–71.
[31] Akhtar J, Amin NS. A review on operating parameters for optimum liquid oil yield in biomass pyrolysis. Renew Sustain Energy Rev 2012;16(7):5101–9.
[32] Mohan D, Pittman CU, Steele PH. Pyrolysis of wood/biomass for bio-oil: a critical review. Energy Fuels 2006;20(3):848–89.
[33] Gelest I. Applying a silane coupling agent. < https://www.gelest.com/wp-content/uploads/09Apply.pdf > [accessed March 5].
[34] Muley PD, Henkel C, Abdollahi KK, Boldor D. Pyrolysis and catalytic upgrading of pinewood sawdust using an induction heating reactor. Energy Fuels 2015;29(11):7375–85.
[35] Guisbiers G, Buchaillot L. Modeling the melting enthalpy of nanomaterials. J Phys Chem C 2009;113(9):3566–8.
[36] Sutherland J, Smith P, Chen J. Quantification of differential diffusion in non-premixed systems. Combust Theor Model 2005;9(2):365–83.
[37] Jang YH, Barber J, Hu SJ. Electrical conductance between conductors with dissimilar temperature-dependent material properties. J Phys D Appl Phys 1998;31(22):3197.
[38] Siakavellas N, Tsopelas N. Detection of the interface between two metals by eddy current thermography. Nondestruct Test Eval 2015;30(3):252–76.
[39] Mortensen PM, Grunwaldt J-D, Jensen PA, Knudsen K, Jensen AD. A review of catalytic upgrading of bio-oil to engine fuels. Appl Catal A 2011;407(1–2):1–19.
[40] McCullen E, Hsu C-L, Tobin R. Electron density changes and the surface resistivity of thin metal films: oxygen on Cu (1 0 0). Surf Sci 2001;481(1–3):198–204.